Residual stresses and practical adhesion: effect of organo-metallic complex formation and crystallization

MAËLENN AUFRAY * and ALAIN ANDRÉ ROCHE †

INSA de Lyon, Laboratoire des Matériaux Macromoléculaires (IMP/LMM), Bâtiment Jules Verne, 17 rue Jean Capelle, F-69621 Villeurbanne Cedex, France

Abstract—Epoxy-amine liquid pre-polymers are often applied onto metallic substrates and cured to obtain painted materials or bonded joint structures. The overall performance of such systems depends on the interphase created between the epoxy-amine polymer and the metallic substrate. When epoxy-amine liquid mixtures are applied onto a metallic oxide layer, concomitant amine chemisorption and oxide dissolution occur leading to organo-metallic complex formation. Depending on the amine nature, as soon as the organo-metallic complex concentration is higher than the solubility product (e.g., isophoronediamine (IPDA)), these organo-metallic complexes crystallize as sharp needles. At the same time, the uncrystallized organo-metallic complexes react with the epoxy monomer to form, after curing cycle, a new network. Moreover, the crystal size increases with the solid/liquid contact time leading to an increase of intrinsic residual stresses and Young's modulus. When aliphatic diethylenetriamine (DETA) was used, no crystallization occurred, but the interphase formation was observed. The aim of this study was to understand and to establish the role of crystallization of organo-metallic complexes formed within the interphase on the practical adhesion performance. As the crystallization of the organo-metallic complex depends on the nature of the amine, two amine hardeners were used (IPDA inducing the formation of crystals and DETA without formation of crystals). For DGEBA-IPDA systems, the ultimate load decreases while residual stresses increase when the liquid/solid contact time increases. When no crystal formation was observed (e.g., DGEBA-DETA system), residual stresses, coating Young's modulus and ultimate load values all remained nearly constant irrespective of the liquid/solid contact time.

Keywords: Practical adhesion; residual stresses; epoxy-amine; metal; interphase; crystals; organo-metallic complexes.

---

*To whom correspondence should be addressed. Present address: Universität des Saarlandes, Lehrstuhl Adhäsion und Interphasen in Polymeren, Gebäude C6-3, Postfach 15 11 50, D-66041 Saarbrücken, Germany. Tel.: (49-681) 302-2548; Fax: (49-681) 302-4960; e-mail: maelenn.aufray@gmail.com

†Deceased.

1. INTRODUCTION

Epoxy-amine liquid mixtures are extensively used as adhesives or paints in many industrial applications, such as in aerospace, automotive and electrical industries. Because of their exceptional adhesion performance, they are also used as a primer on metallic surfaces before application of polyurethane or acrylic paint. When they are applied on metallic substrates and cured, the amine liquid monomer reacts with the metallic oxide to form chemical bonds [1]. Therefore, an interphase having specific chemical, physical and mechanical properties (i.e. properties different from bulk polymer properties and substrate properties) was created between the polymer and the substrate [2–10]. Some studies have reported on the influence of the metallic substrate nature on the pre-polymer cross-linking [11] and have determined the molecular structures formed within the interphase region [12–14]. A complete understanding of epoxy/metal adhesion requires a full knowledge of chemical and physical reactions which take place within the polymer/substrate interphase [15, 16]. Thus, the epoxy/metal interphase is a complex region containing gradients of residual stresses and Young's modulus [17] resulting from structural rearrangement, intermolecular and inter-atomic interactions, and diffusion phenomena [15]. The amine dissolves the hydrated metallic oxide layer and, at the same time, chemisorbs on the metal. The amine chemically reacts to form an organometallic complex. The IUPAC (International Union of Pure and Applied Chemistry) definition of a chelate is a molecular entity in which there is the formation of bonds (or other attractive interactions) between two or more separate binding sites within the same ligand and a single central atom. So hereafter, chelate and organometallic complex will be used as synonyms. Then the complexes can react with the epoxy monomer to form a new network or crystallize if the liquid amine contains more solute entities (e.g., the organometallic complexes) dissolved than it would contain under the equilibrium (i.e., in a saturated solution).

Such crystals act as short fibers, varying the mechanical properties of the coatings. Moreover, when epoxy pre-polymers are applied onto metallic substrates and cured, intrinsic and thermal residual stresses develop within the entire organic layer [18, 19]. These residual stresses reduce the practical adhesion [20]. Therefore, the chemical, physical and mechanical properties of these systems were determined and correlated to the formation and/or crystallization of the chelates, as organometallic complexes formed may crystallize or not. This was possible using two amines: the isophorone diamine, which crystallizes after reaction with the metal, and the diethylenetriamine, which does not crystallize.

2. EXPERIMENTAL

2.1. Materials

The metallic substrates used were either 0.230 ± 0.005-mm-thick 5052 or 1.200 ± 0.005-mm-thick 1050 commercial aluminum alloys from Péchiney, France. Alu-

minum sheets were prepared by die-cutting to provide identical sized strips (50 × 10 mm^2). Before any pre-polymer application, the aluminum substrates were ultrasonically cleaned in acetone for 10 min, wiped dry, submerged for 1 h in a sulfochromic solution (250 g l^{-1} pure sulfuric acid, 50 g l^{-1} chromium(VI) oxide and 87.5 g l^{-1} aluminum sulfate octadecahydrate) at 60°C, rinsed in water for 1 min, dipped in deionized water for 5 min and wiped dry.

After the surface treatment, all substrates were stored less than 2 h in an air-conditioned room (20 ± 2°C and 50 ± 5% RH). The epoxy prepolymer used was pure diglycidyl ether of bisphenol A (DGEBA DER 332 from Dow Chemical, MW = 348 g mol^{-1}). The curing agent was either isophoronediamine (IPDA) from Fluka or diethylenetriamine (DETA) from Aldrich. The stoichiometric ratio (a/e = aminohydrogen/epoxy) used in this work was equal to 1. This ratio was calculated using a functionality of 4 for IPDA, 5 for DETA and 2 for the epoxy monomers. Homogeneous mixtures of DGEBA and IPDA or DETA were achieved by stirring in vacuum (≈1 Pa) at room temperature for 2 min to avoid any air-bubble formation. Epoxy-amine mixtures were applied to the treated metal sheets using shims to obtain the desired coating thickness. The cured coating thickness was determined using an automatic film applicator (from Sheen, UK). The coating layer and substrate had the same widths for residual stresses determination.

To follow the chemical reactions between the metallic surface and liquid monomers, leading to the formation of progressively thicker interphase, liquid monomers were kept in contact with the metallic surface for various durations at room temperature before starting the appropriate coating curing cycle (see the variable contact time at room temperature between liquid pre-polymer and solid substrate in Fig. 1).

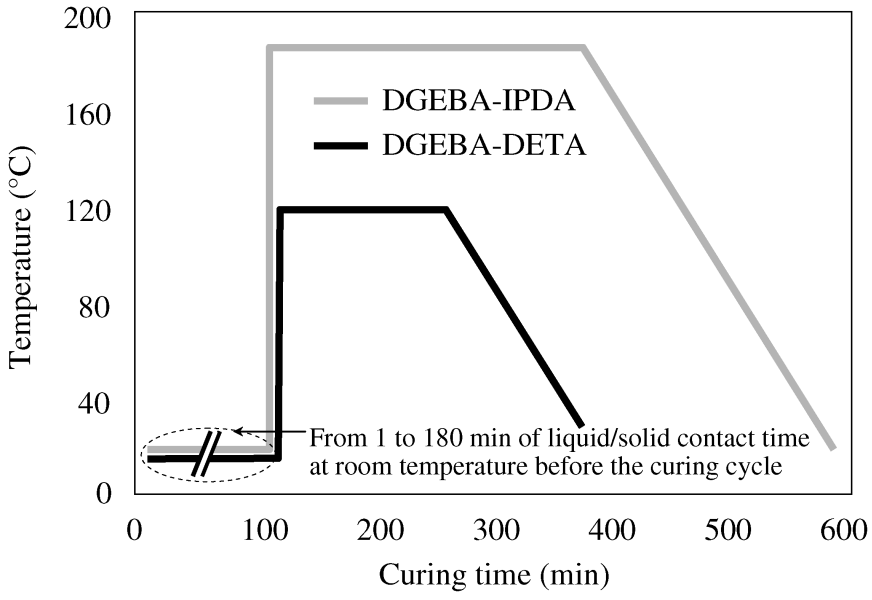

Figure 1. Curing cycles for DGEBA-IPDA and DGEBA-DETA systems.

These curing cycles were used to obtain the maximum conversion of the prepolymer and the maximum glass transition temperature ($T_g = 159°C$ for IPDA and $T_g = 132°C$ for DETA). Conversely, when the interphase formation was not desired, in less than 1 min right after the epoxy-amine application, the coated specimens were placed in the preheated oven.

2.2. Fourier Transform Infra-red spectroscopy (FT-IR)

The pure and modified liquid amines were examined by FT-IR in the transmission mode. The modified amine is the amine monomer which was in contact with a metal for three hours and was then removed to be analyzed. One drop of amine was placed between two KBr pellets in order to be analyzed by FT-IR spectroscopy. The background was recorded using two KBr pellets without anything else as sample. An infrared spectrometer (FT-IR Magna-IR 550 from Nicolet) was used with Omnic FT-IR software. Mid-infrared spectra were recorded in the 400–4000 cm^{-1} range. For each analysis, 128 scans were collected at 4 cm^{-1} resolution.

2.3. Glass transition temperature determination

Differential scanning calorimetry (DSC) experiments were carried out in a Mettler (DSC 30) apparatus to determine the glass transition temperature (T_g) of epoxy networks. Aluminum pans containing 15–20 mg of resin were heated from $-50°C$ to $250°C$ at a heating rate of $10°C\ min^{-1}$ under a continuous flow of argon. The glass transition temperature was determined by the onset point (corresponding to the beginning of the glass transition) with a $\pm 1°C$ sensitivity for coatings of various thicknesses.

2.4. Residual stresses measurement

Experiments were carried out with a flexure machine (FLEX3, Techmétal, Maizières-les-Metz, France) equipped with a 50 N full-scale load cell with a sensitivity of ± 5 mN and a stiffness of $2.2 \times 10^5\ N\ m^{-1}$. One coated sample was tested for each point but the radius of curvature was measured three times for each sample. The error bars presented in the graphs take into account the sensitivity of the load cell and the error in the sample size. After curing (even if the cooling is very slow, in order to prevent the sample from thermal stresses), the samples are elastically deformed and assume a radius of curvature. Coated samples were placed on a planar and rigid stainless-steel substrate. Assuming that the radius of curvature was large compared to both the length and the thickness of the beam, the length of the neutral axis was considered equal to its span. For such a curved sample, and when $\delta \ll L$, the radius of curvature (R_1) is given by:

$$R_1 = \frac{L^2}{8\delta_{max}}, \tag{1}$$

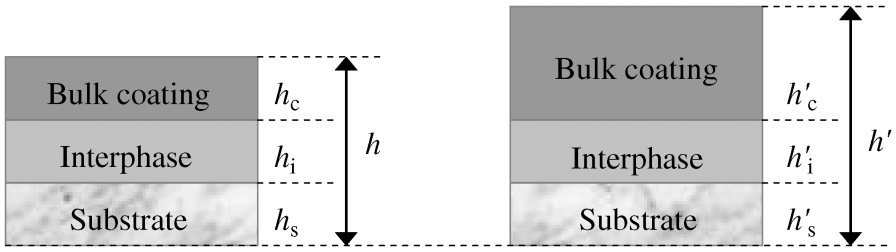

Figure 2. Schematic drawing of two tri-layer models having two different thicknesses (h and h'), but prepared in the same conditions (so $h_s = h'_s$ and $h_i = h'_i$).

where L is the length in mm and δ_{max} is the maximal deflection in mm at the mid-span ($L/2$). The equation developed by Benabdi and Roche [6] takes into account all geometrical and mechanical properties of the sample, such as Young's modulus of the substrate, the interphase and the bulk part of the coating. In order to evaluate the residual stress level at the metal/interphase interface, two different tri-layer systems (i.e., a coated substrate with interphase), presented in Fig. 2, must be considered. These two samples have two different thicknesses, h and h'. Both the epoxy-amine formulation and curing cycle remain constant between the two systems presented in Fig. 2, so it can be assumed that the interphase and metal thicknesses are constant ($h_s = h'_s$ and $h_i = h'_i$). According to Benabdi and Roche [6], the residual stress level at the metal/interphase interface was calculated using equation (2):

$$\sigma = \frac{E_i}{6R_1R'_1(d_{ic}d'_{is} - d'_{ic}d_{is})} \times \frac{A'_{sic}R_1(E_sh_sd_{is} + E_ch_cd_{ic}) - A_{sic}R'_1(E_sh_sd'_{is} + E_ch_cd'_{ic})}{E_sh_s + E_ih_i + E_ch_c}, \quad (2)$$

where:

$E_{s,i,c}$ = Young's modulus of the substrate, the interphase and the bulk coating, respectively

$h_{s,i,c}$ = thickness of the substrate, the interphase and the bulk coating, respectively

h = total thickness ($h = h_s + h_i + h_c$)

R_1 = radius of curvature

$\alpha = E_c/E_s$

$\beta = h_c/h_s$

$d'_{ic} = E_sh_s[E_ih'_i(h_s + h'_i) + E_ch'_c(h' + h'_i)]$

$d'_{is} = E_ch'_c[E_ih'_i(h'_i + h'_c) + E_sh_s(h' + h'_i)]$

$d_{ic} = E_sh_s[E_ih_i(h_s + h_i) + E_ch_c(h + h_i)]$

$d_{is} = E_ch_c[E_ih_i(h_i + h_c) + E_sh_s(h + h_i)]$

$A'_{sic} = E_s^2h_s^4 + E_i^2h_s'^4 + E_c^2h_c'^4 + 12E_sh_sE_ih'_iK'_{is} + 12E_ih'_iE_ch'_cK'_{ic} + 12E_sh_sE_ch'_cK'_{sc}$

$A_{sic} = E_s^2h_s^4 + E_i^2h_s^4 + E_c^2h_c^4 + 12E_sh_sE_ih_iK_{is} + 12E_ih_iE_ch_cK_{ic} + 12E_sh_sE_ch_cK_{sc}$

$K'_{is} = \frac{h_s^2}{3} + \frac{h_sh'_i}{2} + \frac{h_i'^2}{3}$

$K'_{ic} = \frac{h_i'^2}{3} + \frac{h'_ih'_c}{2} + \frac{h_c'^2}{3}$

$$K'_{sc} = \frac{h_s^2}{3} + \frac{h_s h'_c}{2} + \frac{h'^2_c}{3} + h'_i h'$$

2.5. Young's modulus determination

To determine the Young's modulus of coatings, a three-point flexure machine (FLEX3, Techmétal, Maizières-les-Metz, France) was used [21]. The crosshead displacement speed was 0.1 mm min^{-1}. A 50 N full-scale load cell with a sensitivity of ± 5 mN and a stiffness of 2.2×10^5 N m^{-1} was fitted under the crosshead. The load (l) *versus* displacement (δ) curves were recorded. One coated sample was tested for each point but the load versus displacement curve was recorded three times for each sample. The samples were 120 μm thick: therefore, they were considered as bi-layer systems (the coating is here only the interphase: there is no bulk coating). The slopes of the load-displacement curves, within the linear region, were then calculated using a linear regression program. For various span lengths (L_j), the apparent modulus $(E_{app})_j$ values were calculated from the slopes $(1/\delta)_j$ of the load-displacement curves in equation (3):

$$(E_{app})_j I = \frac{L_j^3}{48}\left(\frac{P}{\delta}\right)_j \quad \Longrightarrow \quad (E_{app})_j = \frac{L_j^3}{4bh^3}\left(\frac{P}{\delta}\right)_j, \tag{3}$$

where $I = bh^3/12$ is moment of inertia (b, width of the sample; h, thickness of the sample, $h = h_s + h_c$).

Curves of $(E_{app})_j$ as a function of (h/L_j) were drawn. The ordinate at the origin corresponds to the Young's modulus of the sample (i.e., coated substrate), denoted E_{total} [21]. The Young's modulus of the coating (interphase as the samples are bi-layered systems) was then easily determined by solving equation (4), in the case of a bi-layer system [7–21]:

$$E_c^2(I_c S_c) + E_c(I_c E_s S_s + S_c E_s S_s H - X S_c) - X E_s S_s = 0, \tag{4}$$

where $E_{s,c}$ = Young's modulus of the substrate and the coating, respectively
$I_{s,c} = bh_{s,c}^3/12$ moment of inertia of the substrate and the coating, respectively
$S_{s,c} = bh_{s,c}$ cross-section of the substrate and the coating, respectively
$X = E_{total} I - E_s I_s$
$H = (h_c/2 + h_s/2)^2$

The error bars presented in the graphs take into account the sensitivity of the load cell, the error in the sample size, and the uncertainty in the mathematical regressions (which is the largest error).

2.6. Practical adhesion measurement

The standardized (ISO 14679-1997) three-point flexure test [21, 22] was used to determine the practical adhesion. The three-point flexure test provides a parameter which characterizes the epoxy-amine/metal system practical adhesion and an easily recognizable failure initiation. Of course, for each sample tested,

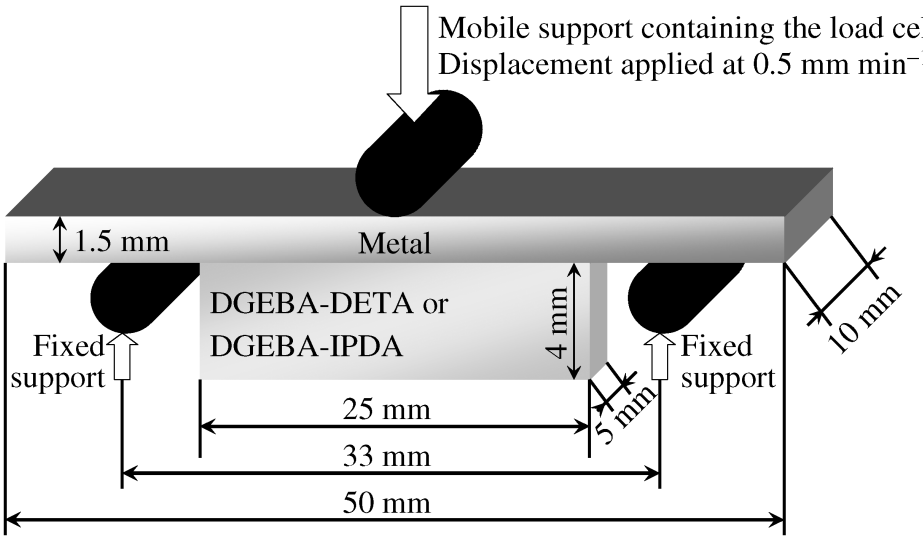

Figure 3. Three-point flexure test.

the failure must be verified as an adhesion failure, and not a cohesive failure. This verification is possible using a microscope: the initiation of the failure must be at the metal/interphase interface, i.e., without any polymer on the metal (as the failure must be an adhesion failure, and if the failure was cohesive, the result was not taken into account in the final average calculation. The epoxy-amine mixtures were applied onto chemically-etched aluminum using a 0.5 ml syringe (Fig. 3). The polymer block formed had the dimensions $25 \times 5 \times 4$ mm^3. This test was performed with a flexure machine (FLEX3, Techmétal, Maizières-les-Metz, France) fitted with a 1000 N full-scale load cell with a sensitivity of ± 0.1 N, a stiffness of 1.1×10^7 N m^{-1} and a cross-head displacement speed of 0.5 mm min^{-1}. The ultimate load ($F_{\max}$, directly measured on the load–displacement curve) was taken as the practical adhesion of epoxy-amine polymers on metallic substrates. A set of six samples was prepared and tested for each data point. The average value of the ultimate load, $F_{\max}$, and its standard deviation (taken as the error in measurement) were determined.

3. RESULTS AND DISCUSSION

In previous works, the mechanisms of the interphase formation when a liquid epoxy (DGEBA)–diamine (IPDA) mixture was applied onto titanium or aluminum alloys [2–4] were determined leading to a better understanding of chemical, physical and mechanical properties of the interfacial region [2–10]. The polymer layer in the substrate surface vicinity has to be considered as an interphase containing gradients of residual stresses and Young's modulus, and where some new chemical species (organo-metallic complexes) and new networks are formed [5–7, 10]. In the following work, the interphase is considered as a third layer of the polymer/substrate system (see Fig. 2), where mechanical, physical and chemical properties are different from those of the bulk polymer.

Bentadjine *et al.* showed that the IPDA reaction with titanium and aluminium led to new peaks in the IR spectra [4]. To confirm that organo-metallic complexes were also formed using DETA as hardener, FT-IR analyses were carried out. Figures 4 and 5 compare the FT-IR spectra of pure and modified amines using IPDA and DETA monomers, respectively. The modified monomer represents the amine applied on the metallic surface and remained in contact with it for 3 h, in order to react with the metal. After 3 h, the modified amine was removed from the surface using a Teflon spatula. In Fig. 4, some new peaks can be observed (for example at 700 cm^{-1} and 820 cm^{-1}), as in Roche *et al.* [3]. For DETA (Fig. 5), only two small peaks appear (at 1660 cm^{-1} and 874 cm^{-1}). In addition, most peaks are displaced

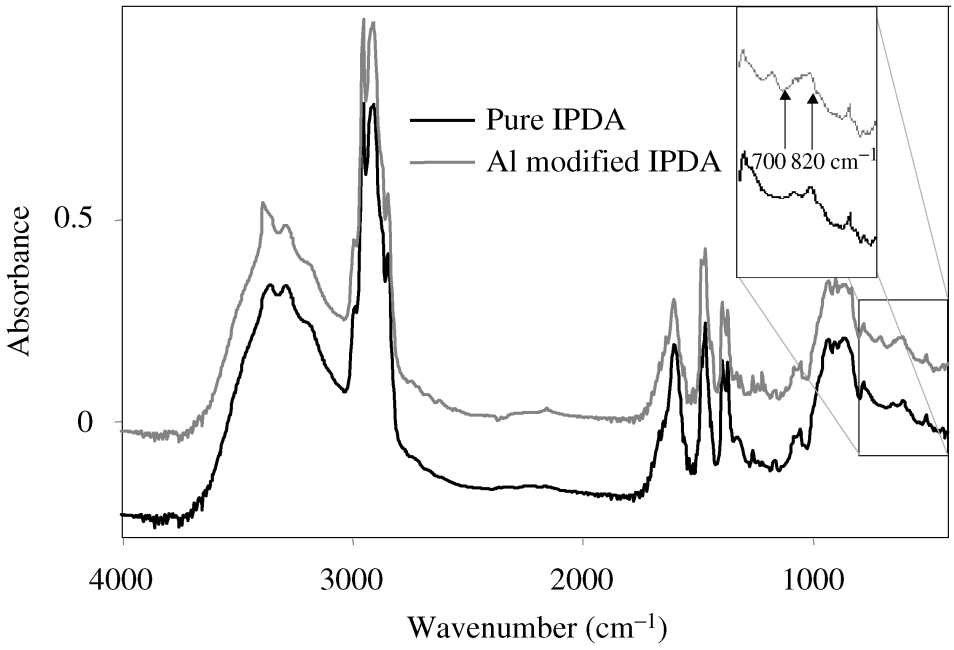

Figure 4. FT-IR spectra of pure and modified IPDA monomers.

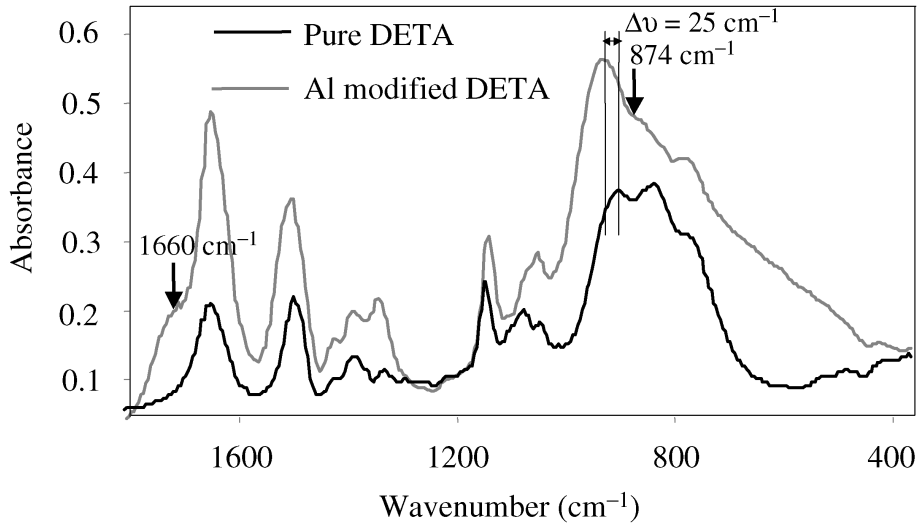

Figure 5. FT-IR spectra of pure and modified DETA monomers.

to the left, which means they all appear at higher wavenumbers (as seen in the example, $\Delta\upsilon = 25\ \mathrm{cm}^{-1}$). Fauquet *et al.* [1] observed the same phenomenon and explained it in terms of molecules changing their conformation when reacting with the metal. We can assume the chelate formation for DETA monomer too, leading to a new DETA conformation, and thus the shift in the FT-IR spectrum.

The interphase thickness was determined by differential scanning calorimetry. Coatings prepared on aluminium and remaining in contact with it for 3 h at room temperature before the curing cycle (in order to produce the maximum interphase thickness) were studied. The T_g value corresponded to the entire coating, and we calculated the glass transition temperature of that part of the coating having a specific thickness (e.g., here h). This glass transition temperature was called the equivalent glass transition temperature ($T_{g,eq}$). Then, two different samples must be considered, having two different thicknesses (h and h') and glass transition temperatures (T_g and T_g'). The $T_{g,eq}$ value was calculated using a mixing law:

$$T_{g,eq} = \frac{h \times T_g - h' \times T_g'}{h - h'}. \tag{5}$$

The variation of $T_{g,eq}$ as a function of the coating thickness is presented in Fig. 6. $I_{g,eq}$ increases when the coating thickness increases until 300 µm for both DGEBA-IPDA and DGEBA-DETA systems. It shows that the interphase thickness is 300 µm for both systems. Moreover, very thin coatings have a very low equivalent glass transition temperature (about 110°C for DGEBA-IPDA system and 90°C for the DGEBA-DETA system, whereas the bulk T_g values are 159°C for the DGEBA-IPDA system and 132°C for the DGEBA-DETA system). Very thick coatings ($h > 300$ µm) have nearly the same glass transition temperature as the bulk material.

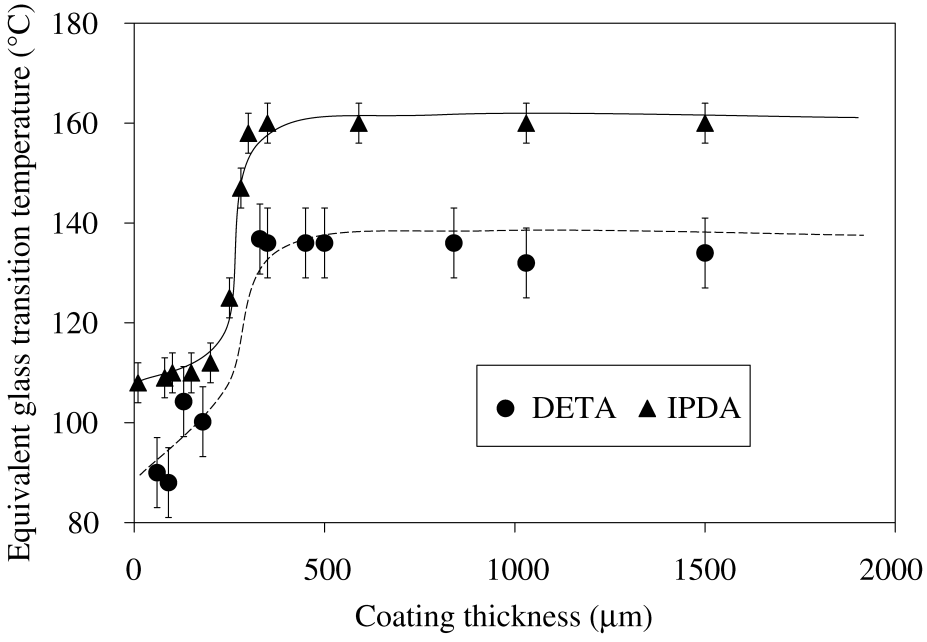

Figure 6. Equivalent glass transition temperature *versus* coating thickness.

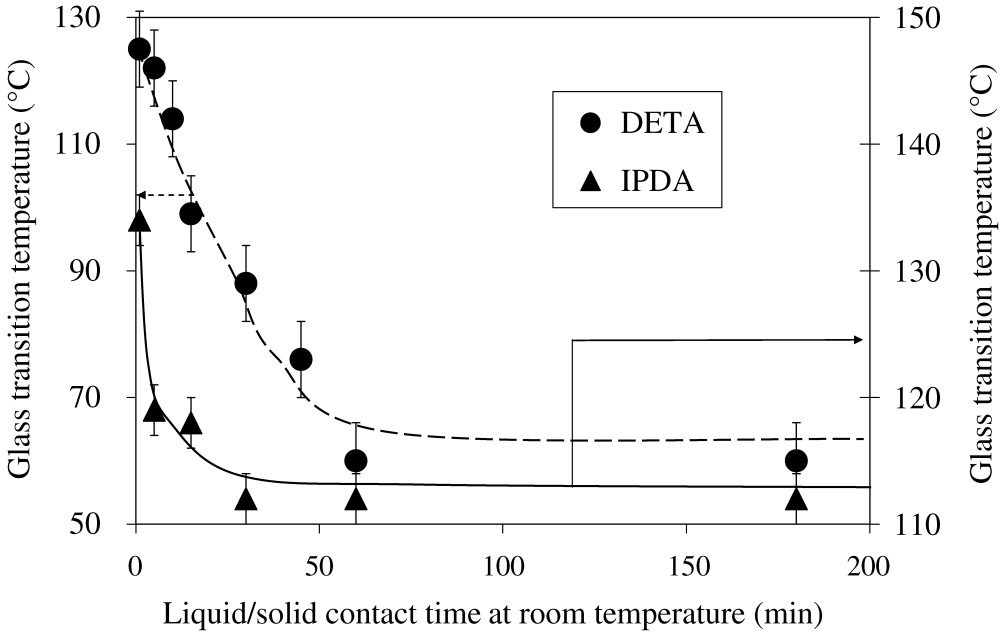

Figure 7. Glass transition temperature for 120-µm-thick coatings *versus* liquid/solid contact time.

In addition to the coating thickness, another very important parameter controlling the interphase formation is the liquid/solid contact time at room temperature before the curing cycle. Indeed polymerization (i.e., reaction between the amine and the epoxy monomers) and interphase formation (i.e., reaction between amine and metal) are in competition, so the variation of the glass transition temperature as a function of the liquid/solid contact time at room temperature before the curing cycle for 120-µm-thick coatings is presented in Fig. 7. For both amines, a decrease of the glass transition temperature is observed as a function of the liquid/solid contact for the first 30 min and after that it remains constant. This means that for both systems, the interphase becomes progressively thicker when the liquid/solid contact time increases up to 30 min. It should be noted that the amine–metal reaction starts as soon as the amine and the metal are in contact at room temperature. This reaction is confirmed as the glass transition temperature is already lower than that of the bulk just after 1 min of contact between the metal and the amine at room temperature (Fig. 7).

The chemical reactions between the metallic surfaces and the amines create residual stresses. These residual stresses are not linked to the cooling of the samples: they are detectable even if samples were cooled very slowly. According to Benabdi and Roche [6, 7] it has been possible to calculate the residual stresses at the interface between the coating and the substrate, from the radius of curvature seen in the coated sample.

The residual stresses at the coating/substrate interface were calculated and plotted as a function of the coating thickness, as well as a function of the liquid/solid contact time for 120-µm-thick coatings (Figs 8 and 9, respectively). The residual stresses decrease when the coating thickness increases, irrespective of the amine used, and

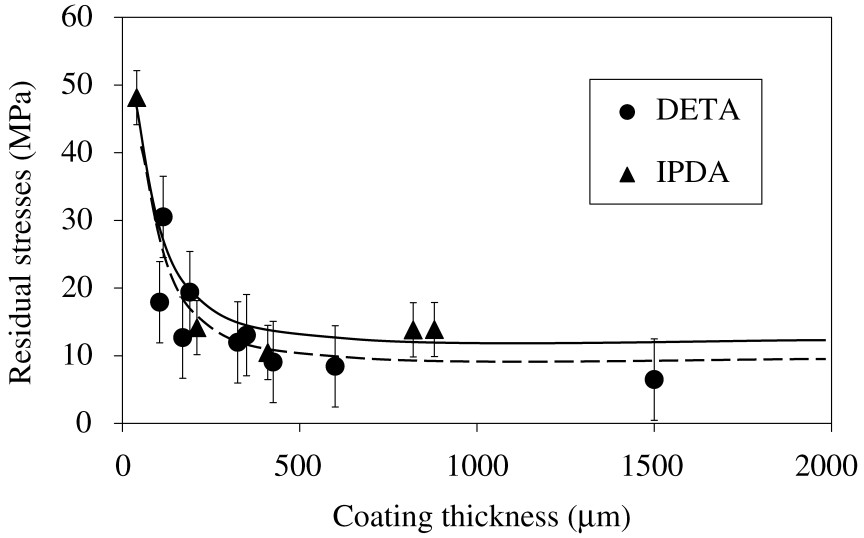

Figure 8. Residual stresses *versus* coating thickness.

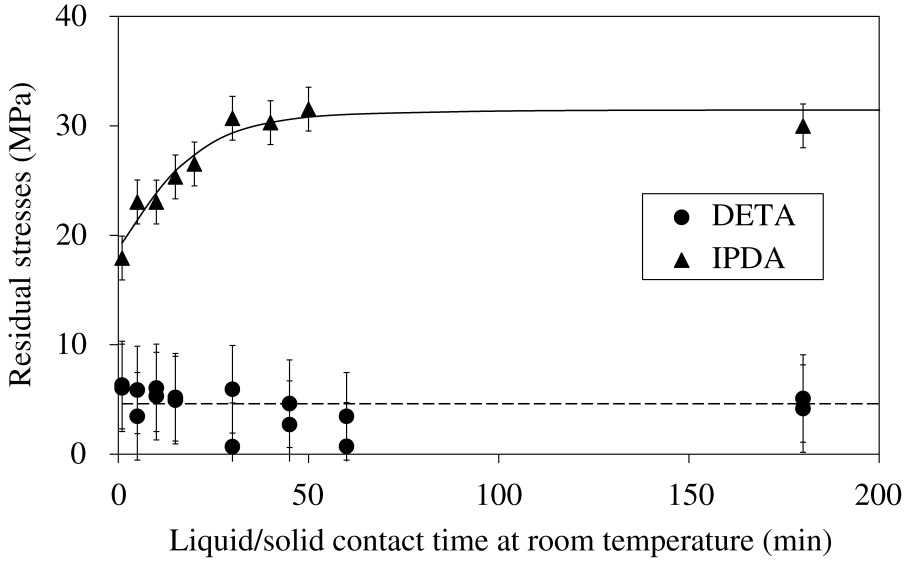

Figure 9. Residual stresses for 120-µm-thick coatings *versus* liquid/solid contact time.

become constant when the coating thickness is higher than 400 µm (as Bouchet *et al.* [5] found previously for the DGEBA-IPDA system).

In addition, for the DGEBA-IPDA system, the residual stresses increase with the interphase formation: they reach a maximum and remain constant after 30 min, when the interphase is completely formed. The increase of the residual stresses is correlated to the increase of the number and the size of the chelate crystals when the liquid-contact time increases as previously reported [3]. Indeed, the interphase becomes anisotropic and inhomogeneous with formation of the crystals. When the DETA hardener is used, residual stresses remain quite constant as a function of the liquid–solid contact time, as the DETA does not crystallize even after three hours in contact with aluminum, as reported before [10]. Residual stress level is lower than for DGEBA-IPDA system.

Table 1.
Young's modulus (E) for pure DGEBA-IPDA and DGEBA-DETA materials and for 120-μm-thick DGEBA-IPDA and DGEBA-DETA coatings

Material	E (GPa)
Bulk DGEBA-IPDA	3.2 ± 0.2
120-μm-thick DGEBA-IPDA coating on Al	10 ± 0.5
Bulk DGEBA-DETA	2.7 ± 0.1
120-μm-thick DGEBA-DETA coating on Al	2.5 ± 0.1

Using the DGEBA-IPDA mixture, applied on an aluminum substrate, Bouchet *et al.* [5] showed that the Young's modulus increased in the metal surface vicinity, irrespective of the surface treatment. Crystals (present in DGEBA-IPDA thin coatings, polymerized on aluminum) act as short fibers and increase the Young's modulus within the interphase. The Young's moduli of DGEBA-IPDA and DGEBA-DETA bulk systems and for 120-μm-thick DGEBA-IPDA and DGEBA-DETA coatings were determined (Table 1). According to Bouchet *et al.* [5], the Young's modulus increases when chelate crystals are formed in DGEBA-IPDA coatings. However, when DETA is used as hardener, no crystals are formed and the Young's modulus of the 120-μm-thick coating decreases slightly, as it is the Young's modulus of the newly formed network and it is slightly lower than the Young's modulus of the initial network.

The Young's modulus can vary with the liquid/solid contact time at room temperature before the curing cycle, as seen for residual stresses so the Young's modulus is plotted as a function of the liquid/solid contact time for 120-μm-thick coatings (Fig. 10). It increases with the interphase formation (i.e., with the increase in the liquid/solid contact time at room temperature before the curing cycle) for the DGEBA-IPDA system. The Young's modulus increases as soon as the liquid/solid contact time at room temperature is longer than 1 min, the same phenomenon was previously seen when the glass transition temperature plotted (Fig. 7). For the DGEBA-DETA system, the Young's modulus decreases when the liquid/solid contact time at room temperature increases, as the newly formed network has its own Young's modulus, which is lower than the Young's modulus of the initial network (pure DGEBA-DETA system, polymerized in the bulk).

Finally, the practical adhesion (determined in terms of the ultimate load) of a 4 mm thick epoxy-amine block was recorded for bi- and tri-layer systems (i.e., without and with interphase, respectively) and correlated to the interphase formation, as shown in Table 2. Both DGEBA-IPDA and DGEBA-DETA systems were investigated, before and after ageing. The ageing was 3-day immersion in deionized water at 40°C. When the interphase is formed, the practical adhesion is constant for the DGEBA-DETA system (the small decrease is within the measurement error), whereas the practical adhesion decreases significantly for the DGEBA-IPDA system. This decrease is linked to the increase of the residual stresses (Fig. 9). After ageing, for both DGEBA-IPDA and DETA systems, the practical adhesion is higher

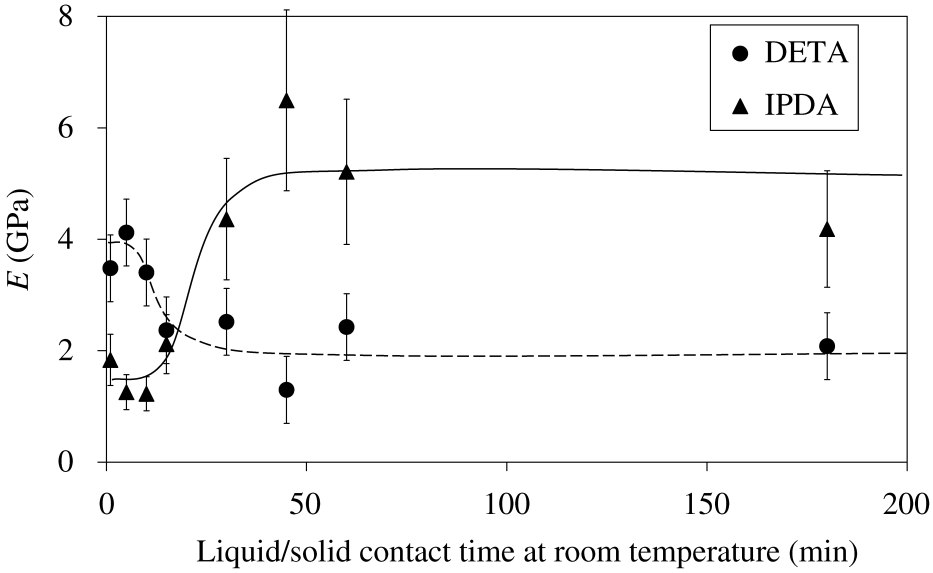

Figure 10. Young's modulus for 120-µm-thick coatings *versus* liquid/solid contact time.

Table 2.
Practical adhesion (in terms of ultimate load, F_{max}) for systems with or without interphase, before and after ageing (3-day immersion in deionized water at 40°C)

	DGEBA-DETA	Aged DGEBA-DETA	DGEBA-IPDA	Aged DGEBA-IPDA
F_{max} (N) with interphase	189 ± 20	142 ± 15	154 ± 16	197 ± 21
F_{max} (N) without interphase	205 ± 21	195 ± 15	180 ± 16	220 ± 22

without any contact between the pre-polymer and the metal at room temperature before the curing cycle (i.e., without any interphase formation) than maintaining the sample for 3 h at room temperature before the curing cycle (i.e., with the interphase formation). Of course, during ageing, the adhesive absorbed water and became plasticized (leading to a decrease of the modulus). But, as the epoxy-amine system polymerized on the metal substrate was a 4-mm-thick block, its stiffness remained infinite, even if the Young's modulus decreased. So the variation of the ultimate load was not affected by the decrease of the Young's modulus. The failure was located at the interphase/metal interface, for both samples with and without ageing. Finally aged and un-aged samples are compared, and for the DGEBA-IPDA system, a significant increase of the practical adhesion is observed after ageing (particularly on samples with interphase). Montois and co-workers had already observed such phenomenon [8, 9] on titanium. As the most important difference between the DETA and the IPDA is the crystallization of the organo-metallic complexes for the IPDA, these crystals could be imagined as an organo-metallic complexes reservoir. The crystallized organo-metallic complexes cannot react with the epoxy monomers: they can be dissolved by the water during ageing, and act as ageing inhibitor. Thus, the best performances are obtained when the organo-metallic complexes (chelates)

are formed without their crystallization (using the DETA as hardener) if the final material does not have to be aged. The IPDA-hardener is very useful if the final material is to be aged, as its practical adhesion will increase after ageing.

4. CONCLUSIONS

When epoxy-amine pre-polymers are applied onto metallic substrates, an interphase is created between the coating part with bulk properties and the metallic surface. A partial dissolution of the metal oxide is observed. Then, metallic ions diffuse in the liquid monomers mixture (epoxy-amine) and react with the amine groups of either IPDA or DETA monomers to form organo-metallic complexes. When the complex concentration is higher than the solubility product, these complexes crystallize as sharp needles (for IPDA). Crystals act as short fibers in an organic matrix leading to an increase of the mechanical properties: The Young's modulus increases for DGEBA-IPDA system. At the same time, for DGEBA-IPDA system, the practical adhesion decreases because of the increase of the residual stresses when the interphase is formed. All the variations in the mechanical properties were linked to the crystals formation, as for DGEBA-DETA system Young's modulus decreases, practical adhesion decreases slightly and residual stresses remain nearly constant. But in both cases (DGEBA-DETA and DGEBA-IPDA systems) interphase was formed during the curing cycle, as the formation of a new epoxy network having a lower T_g was observed.

Acknowledgements

Part of this work was presented at Swiss-Bonding 2003, Rapperswil (Switzerland), May 20–22, 2003.

REFERENCES

1. C. Fauquet, P. Dubot, L. Minel, M. G. Barthes-Labrousse, M. Rei Vilar and M. Villatte, *Appl. Surface Sci.* **81**, 234 (1994).
2. S. Bentadjine, A. A. Roche and J. Bouchet, in: *Adhesion Aspects of Thin Films,* K. L. Mittal (Ed.), Vol. 1, pp. 239–260. VSP, Utrecht (2001).
3. A. A. Roche, J. Bouchet and S. Bentadjine, *Int. J. Adhesion Adhesives* **22**, 431 (2002).
4. S. Bentadjine, R. Petiaud, A. A. Roche and V. Massardier, *Polymer* **42**, 6271 (2001).
5. J. Bouchet, A. A. Roche and E. Jacquelin, *J. Adhesion Sci. Technol.* **15**, 321 (2001).
6. M. Benabdi and A. A. Roche, *J. Adhesion Sci. Technol.* **11**, 281 (1997).
7. M. Benabdi and A. A. Roche, *J. Adhesion Sci. Technol.* **11**, 373 (1997).
8. P. Montois, V. Nassiet, J. A. Petit and Y. Baziard, *Int. J. Adhesion Adhesives* **26**, 391 (2006).
9. P. Montois, V. Nassiet, J. Evieux, Y. Baziard and J. A. Petit, *Proceedings of Euradh,* Glasgow, pp. 161–164 (2002).
10. M. Aufray and A. A. Roche, in: *Adhesion-Current Research and Applications,* W. Possart (Ed.), pp. 89–102. Wiley-VCH, New York, NY (2005).
11. P. J. Hine, S. El. Muddarris and D. E. Packham, *J. Adhesion Sci. Technol.* **1**, 69 (1987).

12. J. Marsh, L. Minel, M. G. Barthes and D. Gorse, *Appl. Surface Sci.* **133**, 270 (1998).
13. G. S. Crompton, *J. Mater. Sci.* **24**, 1575 (1989).
14. Y. H. Kim, G. F. Walker, J. Kim and J. Park, *J. Adhesion Sci. Technol.* **1**, 331 (1987).
15. K. L. Mittal, in: *Adhesion Measurement of Thin Films, Thick Films and Bulk Coatings*, K. L. Mittal (Ed.), STP 640, pp. 5–17. ASTM, Philadelphia, PA (1978).
16. L. H. Sharpe, *J. Adhesion* **4**, 51 (1972).
17. V. Safavi-Ardebili, A. N. Sinclair and J. K. Spelt, *J. Adhesion* **62**, 93 (1997).
18. F. J. Von Preissing, *J. Appl. Phys.* **66**, 4262 (1989).
19. J. A. Nairn, *Int. J. Adhesion Adhesives* **20**, 59 (2000).
20. M. D. Thouless and H. M. Jensen, *J. Adhesion Sci. Technol.* **8**, 579 (1994).
21. A. A. Roche, F. Gaillard, M. J. Romand and M. VonFahnestock, *J. Adhesion Sci. Technol.* **1**, 145 (1987).
22. A. A. Roche, A. K. Behme and J. S. Solomon, *Int. J. Adhesion Adhesives* **2**, 249 (1982).